Long range filament as a solitary wave

L. M. Kovachev
Institute of Electronics, Bulgarian Academy of Sciences,
Tzarigradcko shossee 72,1784 Sofia, Bulgaria, e-mail:lubomirkovach@yahoo.com

We investigate the propagation in air of laser pulses in linear and nonlinear regime. The mathematical model presented in the paper describes the propagation of pulses with narrow-band spectrum, as well as the evolution of broad-band ones. It is shown that the diffraction of pulses with super-broad spectrum or pulses with a few cycles under the envelope is closer to wave type. For such pulses, a new physical mechanism of balance between non-paraxial diffraction and third order nonlinearity appears. Exact analytical three-dimensional soliton solution in this regime is found. We investigate in more detail the nonlinear third order polarization, taking into account the carrier to envelope phase. This additional phase transforms the third harmonic term to GHz terms, which start to generate radiation when the pulse duration reaches the femtosecond range.

PACS numbers: 42.56.Fx, 42.65.Tg
Keywords: Diffraction and scatering, Optical solitons, nonlinear guided waves

Long range filament as a solitary wave

L. M. Kovachev
Institute of Electronics, Bulgarian Academy of Sciences,
Tzarigradcko shossee 72,1784 Sofia, Bulgaria, e-mail:lubomirkovach@yahoo.com

We investigate the propagation in air of laser pulses in linear and nonlinear regime. The mathematical model presented in the paper describes the propagation of pulses with narrow-band spectrum, as well as the evolution of broad-band ones. It is shown that the diffraction of pulses with super-broad spectrum or pulses with a few cycles under the envelope is closer to wave type. For such pulses, a new physical mechanism of balance between non-paraxial diffraction and third order nonlinearity appears. Exact analytical three-dimensional soliton solution in this regime is found. We investigate in more detail the nonlinear third order polarization, taking into account the carrier to envelope phase. This additional phase transforms the third harmonic term to GHz terms, which start to generate radiation when the pulse duration reaches the femtosecond range.

PACS numbers: 42.56.Fx, 42.65.Tg
Keywords: Diffraction and scatering, Optical solitons, nonlinear guided waves

I. INTRODUCTION

When a femtosecond laser pulse with power above the critical for self-focusing propagates in air, a number of new physical effects have been observed, such as long-range self-channeling [1, 2], coherent and incoherent THz and GHz emission [3–5], asymmetric pulse shaping, super-broad spectra [6, 7, 10–12] and others. A remarkable effect is also that some of the light pulses propagate over distances of several kilometers, preserving their spectrum and shapes [1, 2, 8]. In one typical experiment in the near zone up to $1-3\ m$ from the source, when the pulse's intensity exceeds $I > 10^{12}W/cm^2$, initial self-focusing and self-compressing starts, which leads to enlarging the k_z spectrum to super-broad asymmetric one $\triangle k_z \approx k_0$. The process increases the core intensity up to $10^{14}W/cm^2$, where a short plasma column in the nonlinear focus is observed. Usually the standard model describing the propagation in the near zone is a scalar spatio-temporal nonlinear paraxial equation including in addition terms with plasma ionization, higher order Kerr terms, multiphoton ionization and others [14, 21]. The basic model works well partially in the near zone because of the fact that paraxial approximation is valid only for pulses with narrow-band spectrum $\triangle k_z << k_0$. In the far-away zone plasma generation and higher-order Kerr terms are also included as necessary for the balance between the self-focussing and plasma defocussing and for obtaining long range self-channeling in gases. However, the above explanation of filamentation is difficult to be applied in the far-away zone. The higher-order Kerr terms for pulses with intensities of order of $I \sim 10^{12}W/cm^2$ are also too small to prevent self-focussing. As reviewed in [9, 15–17, 22] the plasma density at long distances from the source is much weaker. There are basically two main characteristics which remain the same at these distances - the superbroad spectrum and the width of the core, while the intensity in a stable filament drops to a value of $10^{12}W/cm^2$. To explain existing of plasma free filamentation some authors extend the basic model to a model, where hot spots can be formed from the energy reservoir onto the plasma [15–17]. The experiments, where observation of long-range self-channeling without ionization was realized [16, 17, 22–24], show the need to change the role of the plasma in the laser filamentation. In addition, there are difficulties with the physical interpretation of the coherent THz radiation as a result of plasma generation. The light pulse near the nonlinear focus emits incoherent and *non-homogenous* plasma [5, 9], while the coherent THz radiation requires *homogenous* plasma with fixed electron density of the order of $10^{16}\ cm^{-13}$. Only homogenous plasma can generate coherent THz emission, but such kind of plasma is absent in the process of filamentation. The contribution from ionization in the far-away zone is negligible [9, 21] and this is the reason to look for other physical mechanism which could lead to emission of coherent THz or GHz radiations. Our analysis of the third order nonlinear polarization of pulses with broadband spectrum indicates that the nonlinear term in the corresponding envelope equation oscillates with frequency proportional to the group and phase velocity difference $\Omega_{nl} = 3(k_0 v_{ph} - v_{gr}\triangle k_z)$. Actually, this is three times the well-known Carrier-to Envelope Phase (CEP) difference [25]. This oscillation induces THz generation, where the generated frequency is exactly $\Omega_{THz} = 93GHz$ for a pulse with superbroad spectrum $\triangle k_z \approx k_0$ with a carrier wavelength of 800 nm. All pointed above contradictions between the latest experiments and the standard model make it necessary to look for other physical mechanisms and a new mathematical model for description of these processes.

In this paper we try to answer the following main question: What will happen in the linear and nonlinear regime of propagation, when the pulse obtains a super-broad spectrum? Solving this problem, we present a mathematical model on the basis of the Amplitude Envelope (AE) equation, up to second order of dispersion, without using paraxial

approximation. The diffraction of pulses with super-broad spectrum or pulses with few cycles under the envelope is closer to wave type [26, 27]. Other important difference from the standard model is in the nonlinear part. We show that if CEP is used, the third order nonlinear term for fs pulses cannot be separated into a self-action and third harmonics (GHz) term. For such pulses, a new physical mechanism of balance between non-paraxial (wave-type diffraction) and third order nonlinearity appears. Exact analytical three-dimensional soliton solution in this regime is found.

II. LINEAR REGIME OF NARROW-BAND AND BROAD-BAND OPTICAL PULSES

The typical core of one single filament in the far-away zone is white and the pulse obtains a super-broad spectrum $\triangle k_z \simeq k_0$. Narrow-band pulses are called those, in which the spectral width $\Delta\lambda_z$ is much smaller than the main wavelength of the laser source λ_0. For spectrally narrow pulse the condition $\Delta k_z << k_0$ is satisfied. The spectrum and the phase of a pulse can be modulated with different optical devices and nonlinear elements. Thus, the width of the spectrum of phase-modulated pulse can exceed the width of the spectrum of the spectrally-limited pulses and can reach values in the range of the wave number of the fundamental laser radiation $\Delta k_z \sim k_0$. Broad-band pulses are called the phase-modulated or spectrally limited ones, whose spectral width is of the order of the wavelength of the laser radiation ($\Delta\lambda_z \sim \lambda_0$ or $\Delta k_z \sim k_0$).

The first problem we try to solve here is: what is the diffraction of broad-band optical pulses? The linearized AE, governing the propagation of laser pulses when the dispersion is limited to second order, is [28]:

$$-2ik_0\left(\frac{\partial A}{\partial z}+\frac{1}{v_{gr}}\frac{\partial A}{\partial t}\right)=\Delta A-\frac{1+\beta}{v_{gr}^2}\frac{\partial^2 A}{\partial t^2}, \tag{1}$$

where $\beta = k"k_0 v_{gr}^2$ is a number representing the influence of the second order dispersion and Δ is the standard 3D Laplace operator . Equation (1) is obtained from the Maxwell's equations for non-stationary optical response and is valid if the higher order dispersion terms are neglected as small ones. This is possible only if the series of $k^2(\omega)$:

$$k^2(\omega)=\frac{\omega^2\varepsilon_0(\omega)}{c^2}=k^2(\omega_0)+\frac{\partial\left(k^2(\omega_0)\right)}{\partial\omega_0}(\omega-\omega_0)+\frac{1}{2}\frac{\partial^2\left(k^2(\omega_0)\right)}{\partial\omega_0^2}(\omega-\omega_0)^2+..., \tag{2}$$

is strongly convergent. The convergence of the series (2) for spectrally limited pulses, propagating in the transparent optical regions of solids materials, liquids and gases, depends on the density of the materials and on the spectral broadening of the pulses. For narrow-band wave packets (more than 10 cycles under the envelope), the series of $k^2(\omega)$ is strongly convergent in air and the third derivative term is smaller than the second derivative term by five to six orders of magnitude. In this case we can cut the series to second derivative in gases, as the next terms in the series contribute very little to the Fourier integrals. When there are $1-6$ cycles under pulse (broad-band spectra), the series of $k^2(\omega)$ is weakly convergent for solids and continue to be *strongly convergent* for gases. Then, for dielectrics we must take into account the dispersion terms of higher order as small parameters, while in air the higher order dispersion terms are still negligible [29]. One alternative approach the including while n(w) in the nonlinear equations for short pulses was realized recently in [30] In addition, even if we use also the variation of second order of the dispersion (from 400 nm up to 1000 nm) in air, the values of the dimensionless dispersion parameter $\beta = k"k_0 v_{gr}^2$ continue to be small in the range $\beta < 10^{-4}$ and one averaged small value can be used. That is why we can use the AE equation (1) in air up to the single-cycle regime.

There are mainly two approximations to the linear part of the standard model of filamentation. The first is simply the paraxial spatio-temporal (PST) envelope equation

$$-2ik_0\left(\frac{\partial A}{\partial z}+\frac{1}{v_{gr}}\frac{\partial A}{\partial t}\right)=\Delta_\perp A-\frac{\beta}{v_{gr}^2}\frac{\partial^2 A}{\partial t^2}, \tag{3}$$

where $\triangle_\perp$ denotes the transverse (x, y) Laplace operator. The second add only a mixed zt term in "local time" coordinate system $z' = z$, $\tau = t - z/v$

$$-2ik_0\frac{\partial A}{\partial z}=\Delta_\perp A-\frac{2}{v_{gr}}\frac{\partial^2 A}{\partial\tau\partial z}-\frac{\beta}{v_{gr}^2}\frac{\partial^2 A}{\partial\tau^2}, \tag{4}$$

Both relies on one approximation realized after neglecting the second derivative in the propagation direction. In order to compare our investigation with these results, we need to rewrite AE equation (1) and PST equation (3) in the same coordinate system. Thus, Eq. (1) becomes:

$$-2ik_0\frac{\partial A}{\partial z}=\Delta_\perp A+\frac{\partial^2 A}{\partial z^2}-\frac{2}{v_{gr}}\frac{\partial^2 A}{\partial\tau\partial z}-\frac{\beta}{v_{gr}^2}\frac{\partial^2 A}{\partial\tau^2}, \tag{5}$$

while Eq. PST (3) is transformed into:

$$-2ik_0\frac{\partial A}{\partial z}=\Delta_\perp A-\frac{\beta}{v_{gr}^2}\frac{\partial^2 A}{\partial\tau^2}, \tag{6}$$

As a next step we try to find a fundamental solution of (5). Since this is a parabolic type equation with low order derivative over z, we apply Fourier transformation to the amplitude function in the form: $\hat{A}\left(k_x,k_y,\triangle\omega,z\right)=FFF\left[A\left(x,y,z,t\right)\right]$, where FFF denotes the 3D Fourier transformation in the x,y,τ space and $\triangle\omega=\omega-\omega_0$; $\triangle k_z=\triangle\omega/v_{gr}$ are the spectral widths in the frequency and wave number domains correspondingly. The following ordinary differential equation in the $(k_x,k_y,\triangle\omega,z)$ space is obtained:

$$-2i\left(k_0-\frac{\triangle\omega}{v_{gr}}\right)\frac{\partial\hat{A}}{\partial z}=-\left(k_x^2+k_y^2-\frac{\beta\triangle\omega^2}{v_{gr}^2}\right)\hat{A}+\frac{\partial^2\hat{A}}{\partial z^2}. \tag{7}$$

Analyzing equation (7), we will estimate where we can reduce the diffraction and dispersion of (5) to the standard spatio-temporal paraxial optics of Eq.(6) and where the paraxial optics does not work. The fundamental solution of Eq.(7) is:

$$\hat{A}\left(k_x,k_y,\triangle\omega,z\right)=\hat{A}\left(k_x,k_y,\triangle\omega,0\right)\times$$
$$\exp\left\{i\left[\left(k_0-\frac{\triangle\omega}{v_{gr}}\right)\pm\sqrt{-\left(k_0-\frac{\triangle\omega}{v_{gr}}\right)^2+k_x^2+k_y^2-\frac{\beta\triangle\omega^2}{v_{gr}^2}}\right]z\right\}. \tag{8}$$

The analysis of the fundamental solution (8) of equation (7) is performed in two basic cases:

a: Narrow band pulses - from nanosecond up to $10-20$ femtosecond laser pulses, where the conditions:

$$\triangle k_z=\frac{\triangle\omega}{v_{gr}}<<k_0;\ \frac{\beta\triangle\omega^2}{v_{gr}^2}\leq k_x^2\sim k_y^2<<k_0^2, \tag{9}$$

are satisfied, and the wave number's difference $k_0-\triangle k_z$ can be replaced by k_0. Using the low order of the Taylor expansion and the minus sign in front of the square root from the initial conditions, the spectral kernel in equation (8) is transformed in a spatio - temporal paraxial spectral kernel of the kind:

$$\hat{A}\left(k_x,k_y,\triangle\omega,z\right)=\hat{A}\left(k_x,k_y,\triangle\omega,0\right)\exp\left[-i\left(\frac{k_x^2+k_y^2-\frac{\beta\triangle\omega^2}{v_{gr}^2}}{2k_0}\right)z\right]. \tag{10}$$

It is clearly seen that the spectral kernel (10), governing the evolution of narrow-band pulses, is simply the spectral kernel of the PST equation (6). Thus, when $k_0>>\triangle k_z$ one spatio-temporal approximation can be used, while the linear equation with mixed term (4) is not correct at all.

If we do not use an initially modulated pulse, the shaping becomes obvious: while the transverse projection of the pulse enlarges by the Fresnel's law, the longitudinal temporal shape will enlarge in the same away, proportionally to the dispersion parameter β. Such transformation of a pulse with initially narrow band spectrum is demonstrated in Fig.1, where the typical Fresnel diffraction of the intensity profile ((x,y) projection) is presented. The numerical experiment is performed for 100 femtosecond Gaussian initial pulse at $\lambda=800$ nm, $\Delta k_z<<k_0$, $z_0=30\mu m$, $r_0(x,y)=60\mu m$, with 37.5 cycles under the envelope propagating in air ($\beta=2.1\times10^{-5}$). The result is obtained by solving numerically the inverse Fourier transform of the fundamental solution (8) of the AE equation in the local time frame (5). The

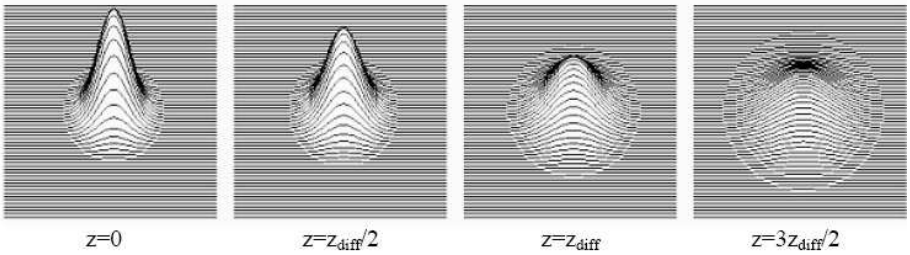

FIG. 1: Plot of the waist (intensity) projection $|A(x,y)|^2$ of a 100 fs Gaussian pulse at $\lambda = 800$ nm, with initial spot $r_0 = 60$ μm, and longitudinal spatial pulse duration $z_0 = 30$ μm, as a solution of the linear equation in local time (5) over distance expressed in diffraction lengths. The spot deformation satisfies the Fresnel diffraction law and on one diffraction length $z = z_{diff}$ the diameter of the spot increases twice, while the maximum of the pulse decreases by the same factor.

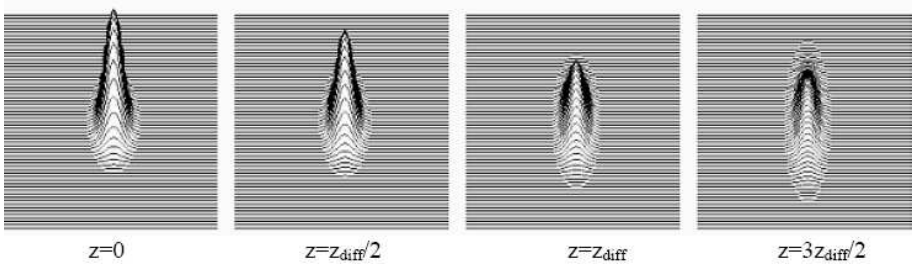

FIG. 2: Side (x,τ) projection of the intensity $|A(x,\tau)|^2$ for the same optical pulse as in Fig. 1. The (x,y) projection of the pulse diffracts considerably following the Fresnel law, while the (τ) projection over several diffraction lengths preserves its initial shape due to the small dispersion.

spot enlarges twice at one diffraction length $z_{diff} = r_0^2 k_0$. Fig. 2 presents the intensity side (x,τ) projection of the same pulse. We should note that while the spot ((x,y) projection) enlarges considerably due to the Fresnel law, the longitudinal time shape (the τ projection) remains the same over several diffraction lengths due to the small dispersion in air.

b: broad band pulses - phase modulated fs pulses or pulses with time duration from attosecond to $10-20$ femtoseconds, where the conditions:

$$\frac{\beta \triangle \omega^2}{v_{gr}^2} \leq k_x^2 \sim k_y^2 \sim (k_0 - \triangle k_z)^2;\ \triangle k_z = \frac{\triangle \omega}{v_{gr}} \simeq k_0, \tag{11}$$

are satisfied.

In air the dispersion parameter is of the order of $\beta = k"k_0 v_{gr}^2 \simeq 2.1 \times 10^{-5}$ and can be neglected. That is why for propagation over several kilometers in air AE (1) can be reduced to the following Diffraction Equation (DE):

$$-2ik_0 \left(\frac{\partial V}{\partial z} + \frac{1}{v_{gr}} \frac{\partial V}{\partial t} \right) = \Delta V - \frac{1}{v_{gr}^2} \frac{\partial^2 V}{\partial t^2}. \tag{12}$$

To find the real diffraction-dispersion picture in 3D space, we solve AE (1) and DE (12) in the same way as in the previous case by applying spatial Fourier transformation to the amplitude functions A and V. The fundamental solutions of the Fourier images $\hat{A}$ and $\hat{V}$ in $(k_x, k_y, \triangle k_z, t)$ space are:

$$\hat{A} = \hat{A}(k_x, k_y, \triangle k_z, t=0) \times$$
$$\exp\left\{ i \frac{v_{gr}}{\beta + 1} \left(k_0 \pm \sqrt{k_0^2 + (\beta+1)\left({k_x}^2 + {k_y}^2 + {\triangle k_z}^2 - 2k_0 \triangle k_z \right)} \right) t \right\}, \tag{13}$$

$$\hat{V} = \hat{V}(k_x, k_y, \triangle k_z, t=0) \exp\left\{ i v_{gr} \left(k_0 \pm \sqrt{{k_x}^2 + {k_y}^2 + (\triangle k_z - k_0)^2} \right) t \right\}, \tag{14}$$

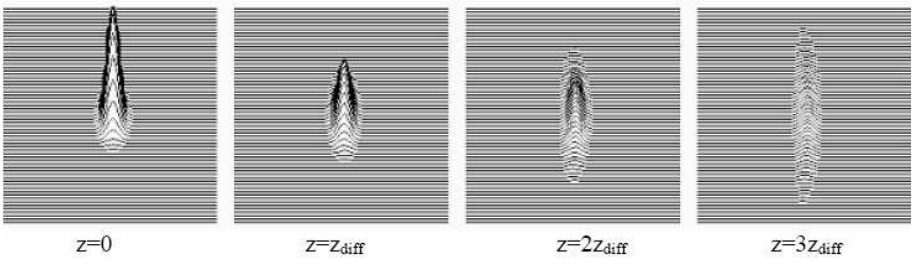

FIG. 3: Evolution of the side (x,z) projection of the intensity $|A(x,z)|^2$ of a 10 fs Gaussian initial pulse at $\lambda = 800$ nm, $\triangle k_z \simeq k_0/3$, $z_0 = r_0/2$, and only 3 cycles under the envelope (large-band pulse $\triangle k_z \approx k_0$), obtained by numerical solving of AE (15) in Galilean frame. At 3 diffraction lengths divergent parabolic type diffraction is observed. In the nonlinear regime a possibility appears: the divergent parabolic type diffraction for large-band pulses to be compensated by the converged parabolic type nonlinear focusing.

respectively. In air $\beta \sim 0$, and the fundamental solution (13) of AE (1) is equal to the fundamental solution (14) of DE (12). That is why in air the diffraction will determine the pulse deformation in the linear regime over a hundred diffraction lengths from the source.

The difference between the main wave number and the spectral width of a large band pulse $(k_0 - \triangle k_z)^2$ is a small number and is of the same order as $k_x^2 \sim k_y^2$. The first important conclusion becomes obvious: For broad-band pulses we cannot replace $(k_0 - \triangle k_z)^2$ with k_0^2 and use Taylor expansion near k_0 for obtaining PST (6) type equation from the spectral kernels in Laboratory (13), Galilean (17) or local time (8) frames. Moreover, the spectral and dimmensionless analysis of the amplitude equation in local time (8) point, that mixed z,t term is of order of second derivative on z direction and one neglecting $\partial^2/\partial z^2$ operator only to obtain Eq. (4) is not correct mathematically. And here appears the first contradiction in the basic model: PST (6) as well as Eq. (4) are used in the linear part of the basic models even when the pulse's spectrum becomes super-broad.

Moreover, the spectral kernels (13), (14) (8) are in square root and we can expect evolution governed by wave diffraction. That is why for broad-band pulses we can expect curvature (parabolic deformation) of the intensity profile of the (x,z) or (x,τ) side projection. It is important to point out that the τ projection in local time coordinates corresponds to the z projection in Laboratory and Galilean frames. The deformation of the pulse is equal in all of these three coordinates with only one difference - while in Lab coordinates the pulse propagates in z direction with group velocity, in Galilean and local frame it stays at one place. That is why, when we discuss the curvature in the side (x,τ) projection of the pulse in local time, this is simply the curvature in (x,z) projection in the Lab and Galilean frames. To investigate the evolution of optical pulses at long distances, it is convenient to rewrite AE (1) and DE (12) in Galilean coordinate system $t' = t; z' = z - v_{gr}t$ respectively:

$$-i\frac{2k_0}{v_{gr}}\frac{\partial A}{\partial t'} = \Delta_\perp A - \beta\frac{\partial^2 A}{\partial z'^2} - \frac{1+\beta}{v_{gr}^2}\left(\frac{\partial^2 A}{\partial t'^2} - 2v_{gr}\frac{\partial^2 A}{\partial t'\partial z'}\right), \tag{15}$$

and for DE we have:

$$-i\frac{2k_0}{v_{gr}^2}\frac{\partial V}{\partial t'} = \Delta_\perp V - \frac{1}{v_{gr}^2}\left(\frac{\partial^2 V}{\partial t'^2} - 2v_{gr}^2\frac{\partial^2 V}{\partial t'\partial z'}\right). \tag{16}$$

The corresponding fundamental solution of AE (15) in Galilean coordinates is:

$$\hat{A}_G(k_x,k_y,\triangle k_z,t) = \hat{A}_G(k_x,k_y,\triangle k_z,t=0)\times$$
$$\exp\left\{i\frac{v_{gr}}{\beta+1}\left[k_0 - (\beta+1)\triangle k_z \pm \sqrt{\left(k_0-(\beta+1)\triangle k_z\right)^2 + (\beta+1)(k_x^2+k_y^2-\beta\triangle k_z^2)}\right]t\right\}, \tag{17}$$

while the fundamental solution of DE (16) becomes:

$$\hat{V}_G = \hat{V}_G(k_x,k_y,\triangle k_z,t=0)\times$$

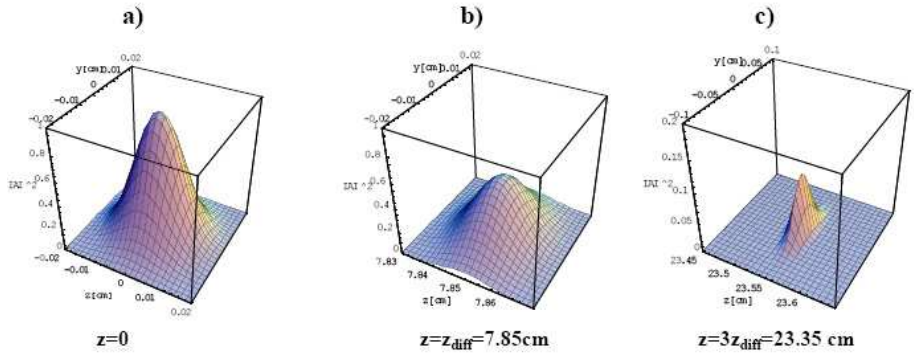

FIG. 4: Fresnel diffraction in air for 330 femtosecond initially non-modulated Gaussian pulse (Fig. 4a) in the form of optical bullet ($t_0 = 330\ fs$; $z_0 = v_{gr}t_0 = r_0 \cong 100\ \mu m$) at a wavelength $\lambda_0 = 800\ nm$, obtained from the exact analytical solution (19) of equation (12). Side projection (y,z) of the intensity of the pulse. At a distance of one diffraction length (Fig. 4b) the amplitude is reduced twice and the half-width in the transverse (x, y) direction enlarges twice. Since dispersion is negligible in the z direction, the pulse preserves its shape. As a result, there is a typical transverse-plane paraxial diffraction optics and optical transformation of a bullet into an optical disk (Fig. 4c).

$$\exp\left\{iv_{gr}\left[k_0 - \triangle k_z \pm \sqrt{\left(k_0 - \triangle k_z\right)^2 + k_x^2 + k_y^2}\right]t\right\}. \tag{18}$$

Fig 3. presents the evolution of the intensity (side (x, z) projection) of a normalized 10 fs Gaussian initial pulse at $\lambda = 800$ nm; $\Delta k_z \simeq k_0/3$; $z_0 = r_0/2$; and only 3 cycles under the envelope (broadband pulse), obtained numerically from AE equation (15) in Galilean frame. The solution confirms the numerically [26] and experimentally [32] observed parabolic type diffraction of broad-band attocecond pulses. And here appears the main physical question for stable pulse propagation in nonlinear regime: Is it possible the divergent parabolic intensity distribution due to non-paraxial diffraction to be compensated by the converging parabolic type nonlinear focusing? If this is the case, then a stable soliton pulse propagation exists. As we show below, only for broad-band pulses one-directional soliton solution of the corresponding nonlinear equations can be found.

We solve analytically the convolution problem (14) for initial Gaussian light bullet of the kind $V(x, y, z, t = 0) = \exp\left(-(x^2 + y^2 + z^2)/2r_0^2\right)$. The corresponding solution is:

$$\begin{aligned} V(x,y,z,t) = \frac{i}{2\hat{r}}\exp\left[-\frac{k_0^2 r_0^2}{2} + ik_0(v_{gr}t - z)\right] \times \\ \left\{i(v_{gr}t + \hat{r})\exp\left[-\frac{1}{2r_0^2}(v_{gr}t + \hat{r})^2\right] erfc\left[\frac{i}{\sqrt{2}r_0}(v_{gr}t + \hat{r})\right]\right. \\ \left. -i(v_{gr}t - \hat{r})\exp\left[-\frac{1}{2r_0^2}(v_{gr}t - \hat{r})^2\right] erfc\left[\frac{i}{\sqrt{2}r_0}(v_{gr}t - \hat{r})\right]\right\}, \end{aligned} \tag{19}$$

where $\hat{r} = \sqrt{x^2 + y^2 + (z - ir_0^2k_0)^2}$. The advantages of this analytical result (19) with respect to the paraxial spatio-temporal approximation is that this solution governs the evolution not only of pulses with many optical cycles under the envelope (paraxial evolution), but also the dynamics of pulses with few-cycles, one-cycle and also sub-cycle regime of propagation. This depends on the values of the (longitudinal) spatial shape r_0 and the main wave number k_0. When their product satisfies $k_0r_0 >> 1$ we are in the regime of typical paraxial Fresnel diffraction (see Fig. 4).

When we have $k_0r_0 \simeq 2\pi$ (few or single-cycle regime) or $k_0r_0 < 2\pi$ (sub-cycle regime), the evolution is closer to wave type diffraction and the pulse shape becomes parabolic at a few diffraction lengths (see Fig. 5).

The analytical solution of DE in Galilean coordinates (16) for initial pulse in the form of a Gaussian bullet is the same as (19), but with a new radial component $\tilde{r} = \sqrt{x^2 + y^2 + (z + v_{gr}t - ir_0^2k_0)^2}$ translated in space and time. The numerical and analytical solutions of AE (1) and DE (12) are equal to the solutions of the equations AE (15) and DE (16) in Galilean coordinates with only one difference: in Laboratory frame the solutions translate in z-direction , while in Galilean frame the solutions stay in the centrum of the coordinate system.

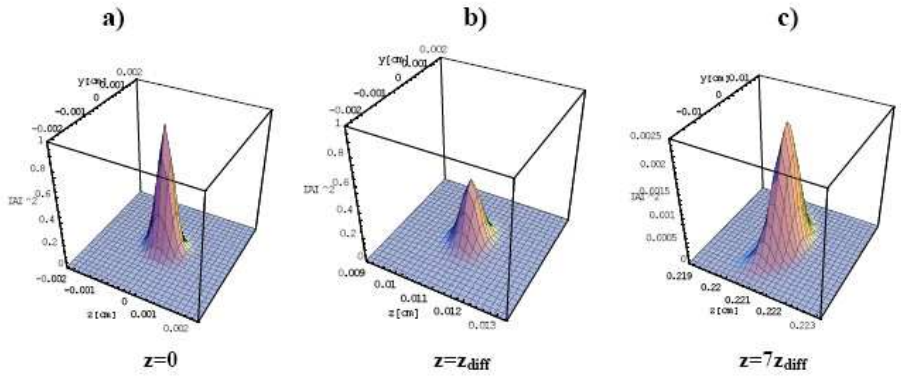

FIG. 5: A type of wave diffraction in air for initial Gaussian pulse with duration of two optical time period - (Fig. 5a) on wavelength $\lambda = 800\ nm$, obtained from the exact analytical solution (19) of equation (12). Side (y,z) projection of evolution of the intensity profile is plotted. On a diffraction length (Fig. 5b) the amplitude decreases again as Fresnel diffraction. The pulse shape takes parabolic profile on few diffraction lengths (see Fig. 5c)

III. A NEW METHOD FOR FINDING EXACT FINITE ENERGY SOLUTION OF THE WAVE EQUATION

Recently in [34] a systematic study was performed on the different kinds of exact solutions and methods for solving the wave equation (20). Here, as in [27], we propose another method. From the wave equation:

$$\Delta E = \frac{1}{v^2}\frac{\partial^2 E}{\partial t^2}, \tag{20}$$

starting with the ansatz:

$$E\left(x,y,z,t\right) = V\left(x,y,z,t\right)\exp\left[-\left(ik_0(z-vt)\right)\right], \tag{21}$$

we separate the main phase and reduce (20) to $3D+1$ parabolic type equation.

$$-2ik_0\left(\frac{\partial V}{\partial z}+\frac{1}{v}\frac{\partial V}{\partial t}\right) = \Delta V - \frac{1}{v^2}\frac{\partial^2 V}{\partial t^2}. \tag{22}$$

Thus, the initial value problem can be solved and fundamental (14), exact (19) or numerical solutions of the corresponding amplitude equation (22) can be obtained. We find a solution of the amplitude equation (22) for initial pulse in the form of a Gaussian bullet (19). Using this method and multiplying (19) with the main phase, we find an exact solution of the wave equation (20):

$$\begin{aligned} E(x,y,z,t) = \frac{i}{2\hat{r}}\exp\left(-\frac{k_0^2 r_0^2}{2}\right)\times \\ \left\{ i(vt+\hat{r})\exp\left[-\frac{1}{2r_0^2}(vt+\hat{r})^2\right] erfc\left[\frac{i}{\sqrt{2}r_0}(vt+\hat{r})\right] \right. \\ \left. -i(vt-\hat{r})\exp\left[-\frac{1}{2r_0^2}(vt-\hat{r})^2\right] erfc\left[\frac{i}{\sqrt{2}r_0}(vt-\hat{r})\right]\right\}. \end{aligned} \tag{23}$$

If substitute the time variable $t=0$ in the solution of the wave equation (23) the initial function of the wave equation transforms to the form $E(x,y,z,0) = \exp(ik_0 z)\exp\left(-(x^2+y^2+z^2)/2r_0^2\right)$. Our analytical and numerical calculations discover that solutions of the wave equation (20) with initial conditions of kind of $E(x,y,z,0) = \exp(ik_0 z)V(x,y,z)$ and initial conditions of kind of $V(x,y,z,0)$ of the corresponding amplitude equations (1) and (22) where V is three dimensional localized smooth function, produced a translation of the solutions in z direction. The wave equation

(20) is hyperbolic type ones, while the amplitude equation (22) is of parabolic type and a initial value problems can be solved (14). And here one method for finding spherically symmetric solutions of the wave equation appear. We present the initial amplitude function V of the amplitude equation as a product of three dimensional localized function, multiplied by plane wave with opposite direction

$$V(x,y,z,0) = \exp(-ik_0 z)G(x,y,z), \tag{24}$$

where G is one spherically symmetric function. The corresponding initial amplitude function of the the wave equation becomes $E(x,y,z,0) = G(x,y,z)$, and practically, solving initial value problem of (22) with initial conditions of kind (24), we can found exact spherically symmetric solutions of the wave equation (20). Here we demonstrate how to obtain with this method the finite energy solution for initial algebraic localized function of the kind

$$G\left(x,y,z,t=0\right) = 1/[1+r^2/r_0^2]. \tag{25}$$

The 3D Fourier expression of (25) in spherical variables is

$$G\left(k_r, t=0\right) = \frac{\pi}{2k_r}\exp\left(-r_0 k_r\right). \tag{26}$$

Hence, the corresponding solution of the amplitude equation after solving the spectral kernels (14) of (22) is

$$V\left(x,y,z,t\right) = \exp\left[-ik_0(z-vt)\right] / \left[\frac{r^2}{r_0^2} + \left(1+\frac{ivt}{r_0}\right)^2\right]. \tag{27}$$

Now again by multiplying with the main phase, the corresponding finite energy solution of the wave equation (20) becomes

$$E\left(x,y,z,t\right) = 1/\left[\frac{r^2}{r_0^2} + \left(1+\frac{ivt}{r_0}\right)^2\right]. \tag{28}$$

A large number of localized finite energy solutions of the wave equation (20) using this method were obtained recently in [35].

IV. NONLINEAR REGIME OF OPTICAL PULSES WITH INITIALLY NARROW BAND SPECTRUM

The laser pulses in a media acquire an additional carrier-to envelope phase (CEP), connected with the group-phase velocity difference. In the linear amplitude equations AE (1) and DE (12) this phase is absent. It can be seen only after multiplication of the solution of the amplitude equation with the main plane wave, propagating with the phase velocity. In one dimensional approximation, an initially *cosine* wave can be written as:

$$E = A\left(z-v_{gr}t\right)\left[\exp ik_0\left(z-v_{ph}t\right) + c.c.\right]/2 = A\left(z-v_{gr}t\right)\cos[k_0\left(z-v_{ph}t\right)], \tag{29}$$

where A is an arbitrary real localized function of z or t. Let us write the expression of the electrical field (29) in Galilean frame $z' = z - v_{gr}t; t' = t$:

$$\begin{aligned} E(z') = A\left(z'\right)\cos\left[k_0 z' - k_0\left(v_{ph}-v_{gr}\right)t\right] = \\ A\left(z'\right)\left(\cos k_0 z' - \omega_{cef}t\right) = A\left(z'\right)\left[\cos(k_0 z')\cos(\omega_{cef}t) + \sin(k_0 z')\sin(\omega_{cef}t)\right], \end{aligned} \tag{30}$$

where the following Carrier to Envelope Frequency (CEF) ω_{cef}, connected with the carrier to envelope phase CEP $\varphi_{cep}(t)$ can be determined:

$$\varphi_{cep} = \omega_{cef}t, \tag{31}$$

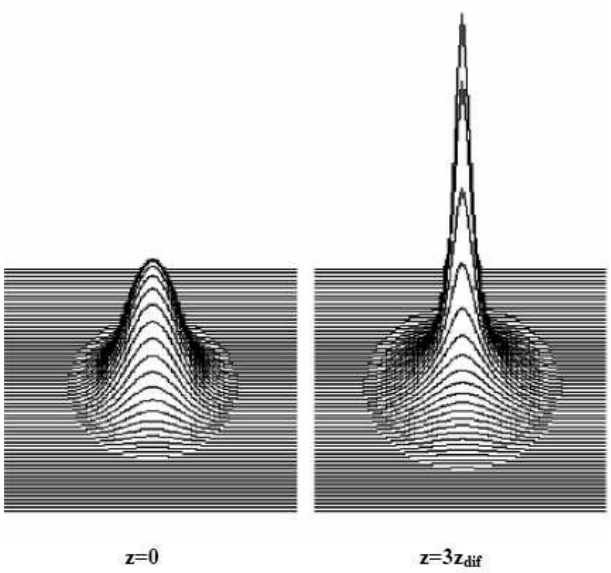

FIG. 6: Evolution of a nanosecond pulse governed by equation (38). The numerical simulation is performed for 1 ns Gaussian pulse at carrying wavelength $\lambda_0 = 800\ nm$ and intensity a little above the critical for self-focusing. The waist (intensity) projection $|V(x,y)|^2$ at initial distance $z = 0$ and distance $z = 3z_{dif}$ is plotted. Typical self-focusing with observing of nonlinear focus and large base is obtained.

$$\omega_{cef} = k_0 \left(v_{ph} - v_{gr}\right). \tag{32}$$

CEF (32) determines the frequency of coincidence between the maximum of the amplitude function, with one of the maxima of the main plane wave in the process of translation of these maxima with respect to the maximum of the envelope with velocity equal to the group - phase velocity difference. When $\varphi_{cep}(t) = 0$ or $\varphi_{cep}(t) = 2n\pi$, there is a coincidence between these two maxima. Generally, the electrical field inside the pulse is not a *cosine* wave, rather it is a *superposition of cosine and sine waves*, determinated by the group-phase velocity difference. It is easy to calculate the CEF for a pulse of TiSa laser at $\lambda_0 = 800\ nm$, propagating in air. For standard atmosphere the result is:

$$\omega_{CEF} \cong 31\ GHz. \tag{33}$$

As mentioned above, the linear complex amplitude equations AE (1) and DE (12) do not depend on this phase. Let us see now what is the influence of this phase on the nonlinear polarization of third order. Following the old tradition from the *CW* nonlinear optics, a *cosine* approximation of the third order polarization without considering CEF is used:

$$\begin{gathered} n_2 E^3\left(x,y,z,t\right) = \vec{x} n_2 \exp\left[i(k_0(z - v_{ph}t)\right] \times \\ \left\{\frac{3}{4}|A|^2 A + \frac{1}{4}\exp\left[2i(k_0(z - v_{ph}t)\right]A^3\right\} + c.c., \end{gathered} \tag{34}$$

The second term in (34) in *CW* approximation corresponds to generation of third harmonics (TH). Most authors neglect this term also in the equations governing the nonlinear pulse propagation, due to the absence of phase velocity mismatching (which is simply CW terminology), and use only the nonlinearity proportional to the intensity (Kerr type). As a further step, the nonlinear equation is usually written in "moving time frame" ($z' = z; t' = t - z/v_{gr}$), which is only a time analog of the standard Galilean transformation ($z' = z - v_{gr}t; t' = t$).

Let us first analyze what happens with the third polarization term in *cosine* approximation written in Galilean frame ($z' = z - v_{gr}t; t' = t$), before neglecting the TH. The CEF (32), being connected with the absolute phase [25], is presented in the phase of the TH term:

$$n_2 E^3\left(x,y,z',t'\right) = n_2 \exp\left[i\left(k_0(z' - (v_{ph} - v_{gr})t'\right)\right] \times$$

$$\left\{\frac{3}{4}|A|^2A+\frac{1}{4}\exp\left[2i\left(k_0(z'-(v_{ph}-v_{gr})t')\right]A^3\right\}+c.c.. \tag{35}$$

Note that the absolute phase is connected with the relative movements with group-phase velocity difference and transforms the TH term into a THz one, with a frequency shift of $\omega_{nl}=3k_0(v_{ph}-v_{gr})\cong 93GHz$ in air of the carrying wavelength $\lambda_0=800nm$. The nonlinear amplitude equation in *cosine* approximation in Laboratory and Galilean frame is:

$$-2ik_0\left(\frac{\partial A}{\partial z}+\frac{1}{v_{gr}}\frac{\partial A}{\partial t}\right)=\Delta A-\frac{1+\beta}{v_{gr}^2}\frac{\partial^2 A}{\partial t^2}+$$
$$n_2k_0^2\left\{\frac{3}{4}|A|^2A+\frac{1}{4}\exp\left[2i(k_0(z-v_{ph}t)\right]A^3\right\}+c.c., \tag{36}$$

and

$$-i\frac{2k_0}{v_{gr}}\frac{\partial V}{\partial t'}=\Delta_\perp V-\frac{1+\beta}{v_{gr}^2}\left(\frac{\partial^2 V}{\partial t'^2}-2v_{gr}\frac{\partial^2 V}{\partial t'\partial z'}\right)+$$
$$n_2k_0^2\left\{\frac{3}{4}|V|^2V+\frac{1}{4}\exp\left[2i\left(k_0(z'-(v_{ph}-v_{gr})t')\right]V^3\right\}+c.c., \tag{37}$$

respectively. As can be seen from (37), the absolute nonlinear frequency shift in air is of the order of $\omega_{nl}\sim 10^{11}\ Hz$, and lies in the spectrum of a fs pulse whose typical frequency width is of the order of $\omega_{fs}\cong 10^{13}-10^{14}\ Hz$. Thus, in the fs region even in *cosine* approximation the TH term is transformed into a THz one and should not be ignored in the corresponding envelope equation (37).

A. Nonlinear propagation of nano and picosecond pulses in air. Self-focusing

Let us first analyze the nonlinear propagation of nanosecond and picosecond pulses. Their frequency widths range from $\omega_{ns}\cong 10^7\ Hz$ up to $\omega_{ps}\cong 10^{10}\ Hz$ for hundred ps pulses if they are not initially modulated. The second nonlinear term in (37) generates one frequency shift $\omega_{nl}\cong 10^{11}\ Hz$, which is bigger than the spectral widths of the pulses. Thus for such pulses the condition for frequency conversion or THz generation is not met, and the second nonlinear THz term can be neglected. Using the results from the previous paragraph for the paraxial character of diffraction for narrow band pulses, Eq.(37) can be written as:

$$-i\frac{2k_0}{v_{gr}}\frac{\partial V}{\partial t'}=\Delta_\perp V-\beta\frac{\partial^2 A}{\partial z'^2}-n_2k_0^2|V|^2V, \tag{38}$$

where the factor 3/4 is included in n_2. The coefficient in front of the second dispersion term from the right side in (38) is of the order of $\beta=k_0v^2k"\sim 10^{-5}$. It is easy to show, that the dispersion term can also be neglected, because the dispersion length for ns and ps pulses in air is from tens up to hundred kilometers, while the diffraction length is of the order of a few tens of centimeters. Naturally the evolution of such long pulses with fiber shape (their longitudinal dimensions are from $0.3-1\ m$ (ps) up to $10-100\ m$ (ns) and their spot is of the order of 100 μm up to $1-2\ cm$) can be governed by a nonlinear equation similar to the equation governing the propagation of optical beams. In Galilean frame there is a diffraction time t_{dif} corresponding to the diffraction length z_{dif} with the relation z_{dif}=$t_{dif}v_{gr}$. We investigate numerically the evolution of a nanosecond pulse governed by equation (38). The numerical simulation is performed for a Gaussian pulse with time duration of 1 ns at carrying wavelength $\lambda_0=800\ nm$ and intensity a little above the critical for self-focusing. Fig 7. shows the nonlinear evolution of the waist (intensity) projection $|A(x,y)|^2$. Typical self-focusing with a nonlinear focus and a large base is obtained.

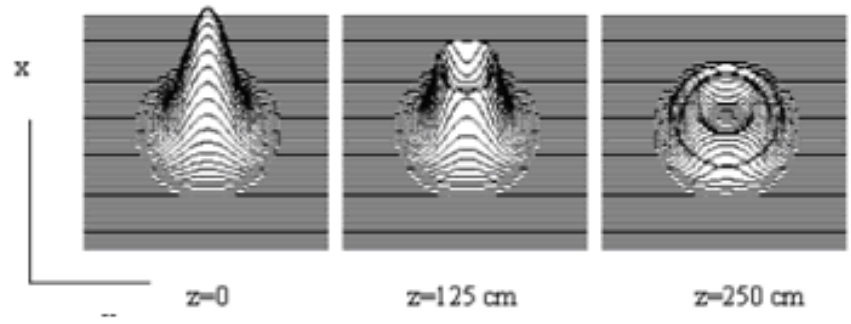

FIG. 7: Nonlinear evolution of the waist (intensity) projection $|V(x,y)|^2$ of a 330 fs initial Gaussian pulse (a1) at $\lambda = 800$ nm, with spot $r_0 = 400$ μm, and longitudinal spatial pulse duration $z_0 = v_{gr}t_0 \cong 100$ μm at distances $z = 0$, $z = 125$ cm, and $z = 250$, obtained by numerical simulation of the 3D+1 nonlinear AE equation (41). The power is above the critical for self-focusing $P = 2P_{kr}$. Typical self-focal zone (core) surrounded by rings is obtained.

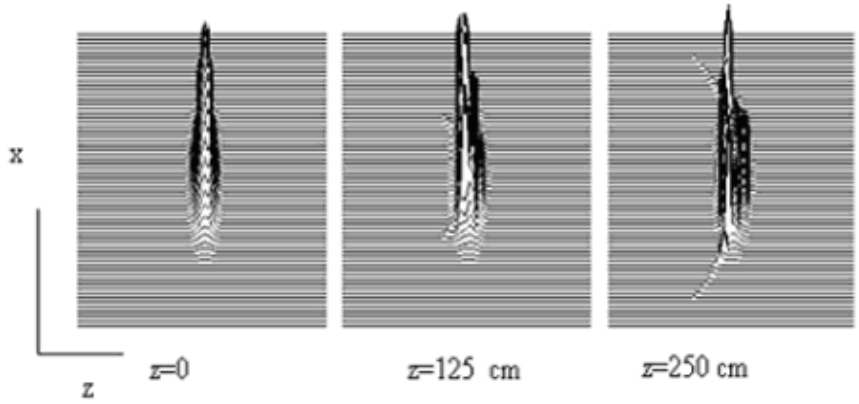

FIG. 8: Numerical simulation of the evolution of the (x,t=z) projection $|A(x,z')|^2$ of the same pulse of Fig. 7 at the same distances, governed by the (3D+1) nonlinear AE equation (41) and the ionization-free model. A self-compression, splitting of the initial pulse to several maxima and X shape deformation is observed.

B. Nonlinear propagation of femtosecond pulses in air. Conical emission and asymmetric spectral broadening

The frequency width of one non-modulated fs pulse is in range $\omega_{fs} \cong 10^{12} - 10^{14}$ Hz. Comparing it with the nonlinear shift $\omega_{nl} \cong 10^{11}$ Hz of the second nonlinear term in (37), it is clearly seen that the THz nonlinear generation lies in the spectral band of a fs pulse and starts to enlarge its spectrum towards high frequencies and short wavelengths. Such deformation of the spectrum of fs pulses in the nonlinear regime is indeed observed in experiments [12, 31]. The THz term emitted in the intensity spectrum of a fs pulse and change the intensity profile, while the *cosine* approximation, separates the nonlinearity into two independent parts, one proportional to the intensity and other response for THz generation. That is why we can expect that a *superposition of cosine and sine wave* under the envelope describe more accurately the pulse propagation. The simplest presentation of such superposition is to write down the the complex electrical field in the form:

$$E(x,y,z,t) = A(x,y,z,t)\exp\left[-ik_0(z - v_{ph}t)\right] = A(x,y,z,t)\left\{\cos\left[k_0(z - v_{ph}t)\right] - i\sin\left[k_0(z - v_{ph}t)\right]\right\}. \quad (39)$$

Substituting expression (39) in the Maxwell equations of an isotropic medium with non-stationary linear and nonlinear response, following standard procedure, we obtain the envelope equations in Laboratory frame ($\beta \cong 0$):

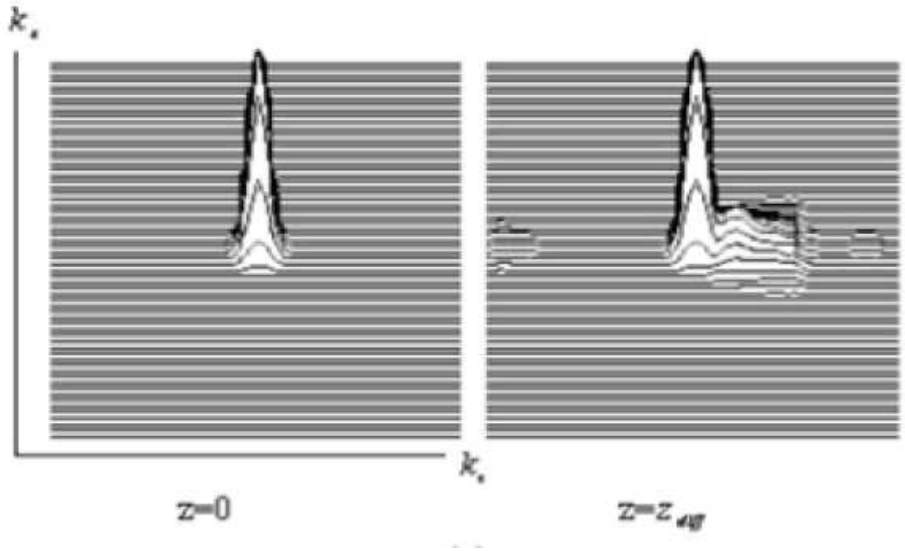

FIG. 9: (a) Typical Fourier spectrum of the side (x, z) projection of the intensity of a pulse in the form of an optical bullet $|A(k_x, k_z)|^2(r_0 = z_0 = 100\ \mu m,\ t_0 330\ fs)$. At several diffraction lengths the pulse enlarges asymmetrically towards the short wavelengths (high k_z wave-numbers).

$$-2ik_0\left(\frac{\partial A}{\partial z}+\frac{1}{v_{gr}}\frac{\partial A}{\partial t}\right)=\Delta A-\frac{1}{v_{gr}^2}\frac{\partial^2 A}{\partial t^2}+n_2k_0^2\exp\left[2i\left(k_0(z-v_{ph}t)\right]A^3,\right. \tag{40}$$

and in Galilean frame:

$$-2i\frac{k_0}{v_{gr}}\frac{\partial V}{\partial t'}=\Delta_\perp V-\frac{1}{v_{gr}^2}\left(\frac{\partial^2 V}{\partial t'^2}-2v_{gr}\frac{\partial^2 V}{\partial t'\partial z'}\right)+n_2k_0^2\exp\left[2i\left(k_0z'-k_0(v_{ph}-v_{gr})t'\right)\right]V^3, \tag{41}$$

are obtained. The entire nonlinear term of these equations oscillates with ω_{nl} and as suggested in the beginning of this subsection, cannot be divided into two parts. Such type of nonlinearity for fs pulses was discussed earlier in [41]. This nonlinear phase is not seen directly in Eq. (40) in Lab coordinates, but if we introduce the phase $\exp[ik_0(z - v_{gr})t]$, associated with the translation in z direction of the pulse, the exact expression of the nonlinear frequency shift is immediately obtained. In our numerical solutions, obtained with equal initial conditions of the equations in Lab (40) and Galilean frames (41), the deformation of the spectral and shape characteristics are the same, with only one difference - translation of the pulse in Lab coordinates and stationarity in Galilean. This is an additional confirmation of the existence of this absolute nonlinear phase in both coordinates. In nonlinear regime, the fs pulses at short distances get super-broad spectra, so an additional approximation of these equations to spatio-temporal paraxial form will not be correct. We use the AE equation (41) to simulate the propagation of a fs pulse, typical for laboratory-scale experiments: initial power $P = 2P_{kr}$, central wavelength $\lambda = 800\ nm$, initial time duration $t_0 = 330\ fs$, corresponding to spatial pulse duration $z_0 = v_{gr}t_0 \cong 100\ \mu m$, and waist $r_0 = 400\ \mu m$. In Fig.7 deformation of the spot $|V(x, y)|^2$ at three different distances from the source, initial $z = 0$, $z = 125\ cm$, and $z = 250\ cm$ is presented. As a result, we obtain the well known self-focal zone (core) with colored ring around, observed in several experiments. The $3D + 1$ nonlinear AE equation (41) gives an additional possibility for investigating the evolution of the side projection of the intensity $|A(x, z')|^2$ profile. The side projection $|V(x, z')|^2$ of the same pulse is presented in Fig.8. The initial Gaussian pulse begins to self-compress at about two diffraction lengths and an X shape deformation is obtained. Fig. 9 presents the typical evolution of the Fourier spectrum of the side projection $|V(k_x, k_{z'}|^2$. At two diffraction lengths the pulse enlarges asymmetrically towards the short wavelengths (high wave-numbers). As seen from our numerical calculations and the comparison with experimental results of other authors [36–38], the non-paraxial ionization-free model (40) and (41) is in good agreement with the experiments on spatial and spectral transformations of a fs pulse in a regime near the critical $P \geq P_{cr}$. Such transformation of the shape and spectrum of fs pulses is typical in the near zone, up to several diffraction lengths, where the conditions for initially narrow-band pulse are satisfied $\triangle k_z << k_0$.

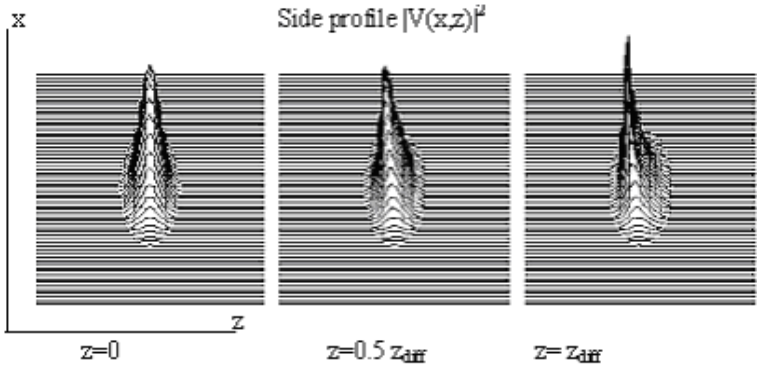

FIG. 10: Numerical simulations for an initial Gaussian pulse with super-broad spectrum $\triangle k_z \approx k_0$ governed by the nonlinear equation (45). The power is slightly above the critical $P = 2P_{kr}$. The side projection $|V(x,z')|^2$ of the intensity is plotted. Instead of splitting into a series of several maxima, the pulse transforms its shape into a Lorentzian of the kind $V(x,y,z') \simeq 1/[1+x^2+y^2+(z'+ia)^2+a^2]$.

V. NONLINEAR PROPAGATION OF BROAD-BAND OPTICAL PULSES. SOLITON REGIME

As demonstrated in the previous section, when a fs pulse with power a little above the critical for self-focusing propagates in air, its spectrum enlarges considerably at short distances and approaches a value of $\Delta k_z \simeq k_0$. One of the basic experimental results in the far-field zone is the observation of stable single pulse with white spectrum. In the experiments also a significant improvement of the pulse quality [39] was observed. The pulse preserves its spectrum $\Delta k_z = k_0 - k_z$, $\Delta\omega = \omega_0 - \omega$, $\Delta\omega/\Delta k_z = v_{gr}$ and shape over significant distances of several kilometers [2, 8]. The preservation of the spectral characteristics means existence of a constant phase during the propagation - $\exp\left[i\Delta k_z\left(z - v_{gr}t\right)\right]$, when we look for a possible soliton regime of propagation. To see the difference between the evolution of narrow-band $\Delta k_z << k_0$ and broadband $\Delta k_z \simeq k_0$ pulses, it is convenient to rewrite the amplitude function, using this constant phase. In spite of the super-broad spectrum, the dispersion parameter in the transparency region from 400 nm up to 800 nm continues to be small, in the range of $\beta \approx 10^{-4} - 10^{-5}$. In Lab frame the phase is:

$$A\left(x,y,z,t\right) = B_0 B\left(x,y,z,t\right)\exp\left(-i(\triangle k_z(z - v_{gr}t)\right), \tag{42}$$

while in Galilean coordinates it is equal to:

$$V\left(x,y,z',t'\right) = B_0 G\left(x,y,z',t'\right)\exp\left(-i\triangle k_z z'\right). \tag{43}$$

The nonlinear amplitude equation for pulses with super-broad spectrum in Laboratory system becomes:

$$-2i(k_0 - \triangle k_z)\left(\frac{\partial B}{\partial z} + \frac{1}{v_{gr}}\frac{\partial B}{\partial t}\right) = \Delta B - \frac{1}{v_{gr}^2}\frac{\partial^2 B}{\partial t^2} + n_2 k_0^2 \exp\left[2i\left((k_0 - \triangle k_z)z - (k_0 v_{ph} - \triangle k_z v_{gr})t\right)\right]B^3, \tag{44}$$

and in Galilean frame it is:

$$-i\frac{(k_0 - \triangle k_z)}{v_{gr}}\frac{\partial G}{\partial t'} = \Delta_\perp G - \frac{1}{v_{gr}^2}\left(\frac{\partial^2 G}{\partial t'^2} - 2v_{gr}\frac{\partial^2 G}{\partial t'\partial z'}\right) + n_2 k_0^2 \exp\left[2i\left((k_0 - \triangle k_z)z' - k_0(v_{ph} - v_{gr})t'\right)\right]G^3, \tag{45}$$

where $\triangle k_z - k_0$ is a very small number or zero. It can be seen that the nonlinear phases in both coordinate systems are equal after the transformation $z' = z - v_{gr}t;\ t' = t$:

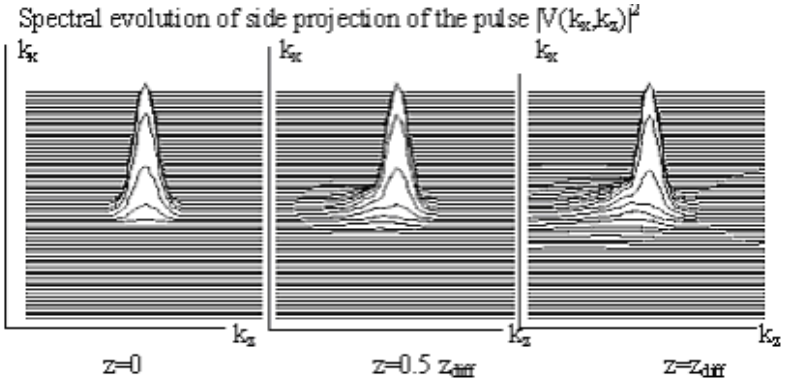

FIG. 11: The evolution of the spectrum $|V(k_x, k_z)|^2$ of the same side intensity projection $|V(x, z')|^2$. The spectrum enlarges towards small k_z wave-numbers (long wavelengths) - typical for Lorentzian profiles.

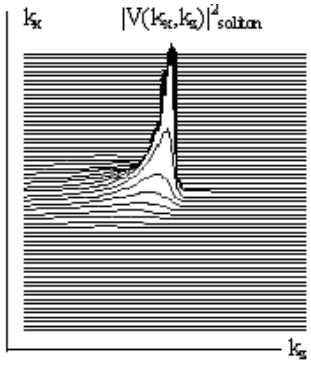

FIG. 12: Plot of the side projection $|V(k_x, k_z|^2$ of the spectrum of a Lorentzian profile $V(x, y, z) = 1/[1+x^2+y^2+(z+ia)^2+a^2]$, $a = 2$ enlarging towards the small k_z wave-numbers (compare with Fig. 8).

$$(k_0 - \triangle k_z)z - (k_0 v_{ph} - \triangle k_z v_{gr})t = (k_0 - \triangle k_z)z' - k_0(v_{ph} - v_{gr})t'. \tag{46}$$

Fig. 10 shows a typical numerical solution of the nonparaxial nonlinear equation (45) (or (44)) for an initial Gaussian pulse with super-broad spectrum $\triangle k_z \approx k_0$. It is obtained by using the split step method (4 step Runge-Kutta method for the nonlinear part). These results are the same both in Laboratory and Galilean coordinate frames, and differ only by a translation term. The side projection $|V(x, z'|^2$ of the intensity profile is plotted for different propagation distances. Instead of splitting into a series of several maxima, the pulse transforms its shape in a Lorentzian form of the kind $V(x, y, z) \simeq 1/[1 + x^2 + y^2 + (z' + ia)^2 + a^2]$. Here, the number a accounts for compression in z' direction and a spatial angular distribution. Fig. 11 presents the evolution of the spectrum $|V(k_x, k_{z'}|^2$ of the side intensity projection for the same pulse. The spectrum enlarges forwards the small k_z wave-numbers (long wavelengths) - typical for Lorentzian type profiles. To compare with Fig. 11, Fig. 12 gives a plot of the side projection $|V(k_x, k'_z|^2$ of the spectrum of a Lorentzian profile $V(x, y, z') = 1/[1 + x^2 + y^2 + (z' + ia)^2 + a^2]$, $a = 2$, enlarging towards the small wave-numbers. The numerical experiments lead to the conclusion that a possible shape of the stable $3D + 1$ soliton can be in the form of a Lorentzian profile. Thus, if we take as an initial condition Lorentzian, instead a Gaussian one, a relative stability in the shape and spectrum can be expected. Fig. 13 shows the evolution of the $|V(x, z'|^2$ profile of a pulse with initial Lorentzian shape $V(x, y, z', t = 0) = 1/[1 + x^2 + y^2 + (z' + ia)^2 + a^2]$, $a = 2$. The pulse propagates over a distance of several diffraction lengths, preserving its initial shape.

A. Spectrally asymmetric 3D+1 soliton solution

The numerical simulations in the previous section for broad-band pulses demonstrate a stable soliton propagation with a specific initial Lorentzian shape. To find an exact soliton solution, we require that a condition of the kind $\triangle k_z = k_0$ is satisfied. The amplitude equation (44) can be rewritten as:

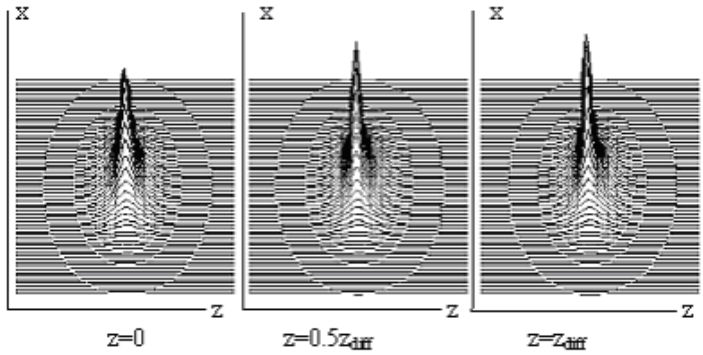

FIG. 13: Evolution of the $|V(x,z'|^2$ profile of a pulse with super-broad spectrum $\triangle k_z \approx k_0$ and initial Lorentzian shape $V(x,y,z',t=0) = 1/([1+x^2+y^2+(z'+ia)^2+a^2]$, $a=2$, governed by the nonlinear equation (45). The pulse propagates over one diffraction length with a relatively stable shape.

$$\Delta B - \frac{1}{v_{gr}^2}\frac{\partial^2 B}{\partial t^2} + k_0^2 n_2 B_0^2 \exp\left[i\left(2\triangle\omega_{nl}t\right)\right]B^3 = 0. \tag{47}$$

To minimize the influence of the GHz oscillation ω_{nl}, we use an amplitude function with a phase opposite to CEP:

$$B(x,y,x,t) = C(x,y,z,t)\exp(-i\triangle\omega_{nl}t). \tag{48}$$

This corresponds to an oscillation of our soliton solution with a frequency $\omega_{nl} \simeq 31$ GHz. Thus, equation (47) becomes:

$$\Delta C - \frac{1}{v_{gr}^2}\frac{\partial^2 C}{\partial t^2} + k_0^2 n_2 B_0^2 C^3 = 2i\frac{\triangle\omega_{nl}}{v_{gr}^2}\frac{\partial C}{\partial t} - \frac{\triangle\omega_{nl}^2}{v_{gr}^2}C \tag{49}$$

To estimate the influence of the different terms on the propagation dynamics, we rewrite equation (49) in a dimensionless form. Substituting:

$$t = t_0 t;\ z = z_0 z;\ x = r_0 x;\ y = r_0 y; \tag{50}$$

$$r_0/z_0 = \delta \sim 1;\ z_0 = v_{gr}t_0;\ t_0 \cong 2\times 10^{-13} - 10^{-14} sec, \tag{51}$$

we obtain the following normalized equation:

$$\Delta C - \frac{\partial^2 C}{\partial t^2} + \gamma C^3 = i\alpha\frac{\partial C}{\partial t} - \beta C, \tag{52}$$

where $\hat{\gamma} = r_0^2 k_0^2 n_2 B_0^2$ is the nonlinear constant, $\alpha = 2\triangle\omega_{nl}r_0^2/v_{gr}^2 t_0$ and $\beta = \triangle\omega_{nl}^2 r_0^2/v_{gr}^2$. For a typical fs laser pulse with a carrier wavelength 800 nm and a spot $r_0 = 100\ \mu m$, the constants of both terms in the r.h.s of equation (52) are very small ($\alpha \sim 10^{-2}$ and $\beta \sim 10^{-4}$) and can be neglected. Thus, equation (52) becomes:

$$\Delta C - \frac{\partial^2 C}{\partial t^2} + \hat{\gamma} C^3 = 0, \tag{53}$$

or coming back to dimensional variables, (53) is simply:

$$\Delta C - \frac{1}{v_{gr}^2}\frac{\partial^2 C}{\partial t^2} + \gamma C^3 = 0, \tag{54}$$

where $\gamma = \hat{\gamma}/r_0^2$. Furthermore, we shall assume that the new envelope wave equation (54) has solutions in the form:

$$C\left(x,y,z,t\right)=C(\tilde{r}), \tag{55}$$

where $\tilde{r}=\sqrt{x^2+y^2+(z+ia)^2-v^2(t+ia/v)^2}$. From the nonlinear wave equation (54), using (55), the following ordinary nonlinear equation is obtained:

$$\frac{3}{\tilde{r}}\frac{\partial C}{\partial\tilde{r}}+\frac{\partial^2 C}{\partial\tilde{r}^2}+\gamma C^3=0. \tag{56}$$

The number a counts for the longitudinal compression and the phase modulation of the pulse. When the nonlinear coefficient is slightly above the critical and reaches the value $\gamma=2$, equation (56) has exact particle-like solution of the form:

$$C=\frac{sech(ln(\tilde{r}))}{\tilde{r}}. \tag{57}$$

Using the fact that $exp(ln(\tilde{r}))=\tilde{r}$ and $exp(-(ln\tilde{r}))=\frac{1}{\tilde{r}}$, the solution (57) is simplified to the following algebraic soliton:

$$C(\tilde{r})=\frac{2}{1+x^2+y^2+(z+ia)^2-v^2(t+ia/v)^2} \tag{58}$$

Solution (58) gives the time evolution of the Lorentz initial shape, investigated in the previous section. As seen from equation (54), the solution appears as a balance between the parabolic (not paraxial) wave type diffraction of a broad-band pulse $\triangle k_z=k_0$, and the nonlinearity of third order. The maxima of this solution are at the points where $\tilde{r}^2=0$. If we solve the second order equation $z^2+2iaz-2iav_{gr}t-v_{gr}^2t^2=0$ on the propagation axes (z,t), only one real solution $z=v_{gr}t$ can be obtained. It corresponds to one-directional propagation with position of the maximum on the z - coordinate $z=v_{gr}t$. Recently, exact solutions of the equation (49) with GHz perturbation term were obtained in [43].

VI. CONCLUSIONS

The femtosecond region is remarkable with the possibility for quick transformation of narrow-band pulses to broad-band ones in nonlinear regime. On the other hand, following the tradition from ns and ps optics, the basic theoretical studies continue to investigate the processes of fs pulses with the corresponding envelope equation for narrow-band laser pulses, working in paraxial approximation and Kerr type nonlinearity. To cover the new effects in the fs region, such as conical emission, coherent THz and GHz radiation, filamentation and long-range wave guiding, more of the authors start to add to this paraxial nonlinear equation terms, corresponding to additional processes, like plasma generation, higher order Kerr terms, optical rectification and others. It is easy to show that plasma generation and higher order Kerr terms are negligible with respect to nonlinearity of third order for pulses with intensities of the order of $I\simeq 10^{12}\ W/cm^2$. This is the typical intensity for observing the above new processes. On the other hand, optical rectification requires the presence of an additional high-power wave at the second harmonics frequency, which is not observed in the experiments. That is why we start to look for theory and equations, which can cover the evolution not only of narrow-band pulses, but also of broad-band ones. In the process of investigation we found also that in the fs region it is not possible to reduce the nonlinearity of third order to Kerr type only (proportional to the intensity). Therefore, as a first step we introduce new linear amplitude equations (1) and DE (12), allowing us to solve numerically and analytically the problem with propagation of pulses with super-broad spectra. Different regimes of diffraction are analyzed. The typical fs pulses up to 20 fs diffract following the Fresnel law in the near zone, in a plane orthogonal to the direction of propagation, while their longitudinal shape is preserved in air or is enlarged a little, due to dispersion. Broad-band pulses (only a few cycles under the envelope or phase-modulated pulses) at several diffraction lengths obtain a parabolic form of the intensity. We solve the convolution problem of the diffraction equation DE (12) for an initial pulse in the form of a Gaussian bullet, and obtain an exact analytical solution (19). A new method for solving evolution problems of the wave equation is also proposed. In the nonlinear regime we investigate more precisely the nonlinear third order polarization, taking the CEP into account. This additional phase transforms the TH term into THz or GHz terms, depending on the spectral width of the pulse. Thus, we propose a new

mechanism of THz and GHz generation from fs pulses in the nonlinear regime. For pulses with power a little above the critical for self-focusing, we investigate two basic cases: pulses with narrow-band spectrum and with broad-band spectrum. The numerical simulation of the evolution of narrow-band pulses (standard 100 fs pulses), gives a typical conical emission and a spectral enlargement to the short wavelengths. Our study of broad-band pulses leads to the conclusion that their propagation is governed by the nonlinear wave equation with third order nonlinear term (54), when the THz oscillation is neglected as a small term. Exact soliton solution of equation (54) is obtained. The soliton appears as a balance between parabolic divergent type wave diffraction and parabolic convergent type of nonlinear self-focusing. Numerically, we demonstrate a relative stability of the soliton with respect to the THz oscillations.

VII. ACKNOWLEDGEMENTS

This work is partially supported by the Bulgarian Science Foundation under grant DO-02-0114/2008.

[1] A. Braun, G. Korn, X. Liu, D. Du, J. Squier, and G. Mourou, Opt. Lett. , 20(1), 73-75 (1995).
[2] L. Wöste, C. Wedekind, H. Wille, P. Rairoux, B. Stein, S. Nikolov, C. Werner, S.Nierdermeier, F. Ronneberger, H. Schillinger, and R. Sauerbrey, AT-Fachverlag, Stuttgard, Laser and Optoelectronik 29, 51-53 (1997).
[3] S. Tzortzakis, G. Méchain, G. Patalano, Y.-B. André, B. Prade, M. Franco, A. Mysyrowicz, J. M. Munier, M. Gheudin, G. Beaudin, and P. Encrenaz, Opt. Lett. , 1944-1946, (2002).
[4] C. D'Amico, A. Houard, M. Franco, B. Prade, A. Mysyrowicz, Optics Express, 15, 15274-15279 (2007).
[5] C. D'Amico, A. Houard, S. Akturk, Y. Liu, J. Le Bloas, M. Franco, B. Prade, A. Couairon, V. T. Tikhonchuk, and A. Mysyrowicz, New J. of Phys., 10, 013015 (2008).
[6] C. P. Hauri, W. Kornelis, F. W. Helbing, A. Couairon, A. Mysyrowicz, J. Biegert, U. Keller, Appl. Phys. B, 79, 673-677 (2004).
[7] C. P. Hauri, A. Guandalini, P. Eckle, W. Kornelis, J. Biegert, U. Keller. Optics Express, 13, 7541 (2005).
[8] G. Méchain, C. D'Amico, Y.-B. André, S. Tzortzakis, M. Franco, B. Prade, A. Mysyrowicz, A. Couairon, E. Salmon, R. Sauerbrey, Opt. Commun. , 247, 171-108 (2005).
[9] G. Méchain, "Study of filamentation of femtosecond laser pulses in air", These de doctorat, Ecole Polytechnique, Palaiseau, France, 2005.
[10] A. Couairon, J. Biegert, C. P. Hauri, W. Kornelis, F. W. Helbing, U. Keller, A. Mysyrowicz, J. Mod. Opt., 53, 75-85 (2006).
[11] S.L. Chin, A. Brodeur, S. Petit, O. G. Kosareva, V. P. Kandidov, J. Nonlinear Opt. Phys. Mater., 8, 121-146 (1998).
[12] J. Kasparian, R. Sauerbrey, D. Mondelain, S. Niedermeier, J. Yu, Y. P. Wolf, Y.-B. André, M. Franco, B. S. Prade, S. Tzortzakis, A. Mysyrowicz, H. Wille, M. Rodriguez, L. Wöste, Opt. Lett. , 25, 1397-1399 (2000).
[13] A. Couairon, and A. Mysyrowicz, Physics Reports, 441, 47-189 (2007).
[14] S. L. Chin, S. A. Hosseini, W. Liu, Q. Luo, F. Théberge, N. Aközbek, A. Becker, V. P. Kandidov, O. G. Kosareva, and H. Schoeder, Can. J. Phys. 83, 863-905 (2005).
[15] V. P. Kandidov, O. G. Kosareva, I. S. Golubtsov, W. Liu, A. Becker, N. Aközbek, C. M. Bowden, and S. L. Chin, Appl. Phys B 77, 149 (2003).
[16] Y. Chen, F. Théberge, O. Kosareva, N. Panov, V. Kandidov, ans S. L. Chin, Optics Letters, 15, 3477-3479 (2007).
[17] J. -F. Daigle, O. Kosareva,N. panov, T. -J. Wang, S. Hosseini, S. Yuan, G. Roy, S.L. Shin, Opt. Comm. 284, 3601 (2011).
[18] Daniele Faccio, Alessandro Averhi, Antonio Lotti, Paolo Di Trapani, Arnaud Couairon, Dimitris Papazoglou, Stelios Tzortzakis, Optics Express, 16 1565-1569 (2008)
[19] M. Kolesik and J. V. Moloney, Optics Express, 16, 2971-2986 (2008).
[20] Y. R. Shen, *The Principles of Nonlinear Optics*,(Wiley-Interscience, New York, 1984).
[21] P. Béjot, J. Kasparian, S. Henin, V. Loriot, T. Viellard, E. Hertz, O. Faucher, B. Lavorel, and J.-P. Wolf, Phys. Rev. Lett., 104, 103903 (2010).
[22] G. Méchain, A. Couairon, Y.-B. André, C. D'Amico, M. Franco, B. Prade, S. Tzortzakis, A. Mysyrowicz, R. Sauerbrey, Appl. Phys B, 79, 379-382 (2004).
[23] A. Dubietis, E. Gaižauskas, G. Tamožauskas, P. Di Trapani, Phys. Rev. Lett 92, 253903 (2004).
[24] Todd A. Pitts, Ting S. Luk, James K. Gruetzner, Thomas R. Nelson, Armon McPherson, Stewart M. Cameron and Aaron C. Bernstein, J. Opt. Soc. Am. B , 21, 2006-2016 (2004).
[25] Martin Wegener, *Extreme Nonlinear Optics*, (Springer-Verlag, Berlin Heidelberg, 2005).
[26] N. M. Naumova, J.A. Nees, I.V.Sokolov, B. Hou, and G. A. Mourou, Phys. Rev. Lett. 92,6, 063902 (2004).
[27] Lubomir M. Kovachev, Kamen Kovachev, J. Opt. Soc. Am. A , 25, 2232-2243 (2008); "Erratum " , 25, 3097-3098 (2008).
[28] Kamen Kovachev and Lubomir Kovachev, "Linear and Nonlinear Femtosecond Optics in Isotropic Media - Ionization Free Filamentation",(Laser System for Application, InTech, Rieka, 209-229 2011).
[29] Kamen Kovachev,"Propagation of ultrashort laser pulses in media with non-stationary optical and magnetic response", (PhD thesys, Sofia University, Sofia, 2011).

[30] Yu. A. Shpolyanskiy, JETP 111, 557-566 (2010).
[31] S. Petit, A. Talebrour, A. Proulx, S.L.Chin, Laser Phys., 10, 93-100 (2000).
[32] N. M. Naumova, J. A. Nees, E. P. Power, and G. A. Mourou, Laser Physics, Vol. 15, No. 6, pp. 832-837 (2005).
[33] T. Brabec, F. Krausz, Phys. Rev. Lett. 78, 3282-3285 (1997).
[34] A. P. Kiselev, Optics and Spectroscopy, 102, 603-622 (2007).
[35] D. A. Georgieva, K. L. Kovachev and L. M. Kovachev, "A new class of exact finite energy solutions of the wave equation", in press.
[36] E. T. J. Nibbering, P.F.Curley, G. Grillon, B.S. Prade, M.A.Franco, F. Salin, A. Mysyrowicz, Opt. Lett., 21, 62-64 (1996).
[37] S. L. Chin, Phys. Can. 60, 273-281 (2004).
[38] D. Aumiler, T. Ban, G. Pichler, Phys.Rev. A, 71, 063803 (2005).
[39] B. Prade, M. Franco, A. Mysyrowicz, A. Couairon, H. Buersing, B. Eberle, M. Krenz, D. Seiffer, O. Vasseur, Opt. Lett., 31, 2601 (2006)
[40] J. Kasparian, R. Sauerbrey, and S. L. Chin, Appl. Phys. B 71, 877-879 (2000).
[41] M. Kolesik, E. M. Wright, A. Becker, and J. V. Moloney, Appl. Phys. B, 85, 531-538 (2006).
[42] L. M. Kovachev, J. Mod. Opt., 56, 1797 - 1803 (2009).
[43] Dakova, D. I., Dakova, A. M. Proceedings of SPIE, 7747, 77471C (2011).

Corresponding author: L. M. Kovachev
Institute of Electronics, Bulgarian Academy of Sciences,
72 Tzarigradcko shossee,1784 Sofia, Bulgaria,
Tel-Fax:+359 2 8601110
e-mail:lubomirkovach@yahoo.com